

Power Electronics Based FACTS Controller for Stability Improvement of a Wind Energy Embedded Distribution System

Sidhartha Panda and N.P.Padhy

Abstract—In recent years generation of electricity using wind power has received considerable attention worldwide. Induction machines are mostly used as generators in wind power based generations. Since induction machines have a stability problem as they draw very large reactive currents during fault condition, reactive power compensation can be provided to improve stability. This paper deals with stability improvement of a distribution system embedded with wind farms by using power electronics based Flexible AC Transmission Systems (FACTS) reactive power compensator controller. The dynamic behavior of the example distribution system, during an external three-phase fault and under various types of wind speed changes, is investigated. The study is carried out by three-phase, non-linear, dynamic simulation of distribution system component models. Simulation results are presented for different cases such as with and without FACTS and also for different modes of operation of FACTS controller. The effect of constant wind speed and linear change in wind speed on stability is also analyzed. The simulation analysis of stability of distributed system with wind farm is performed using MATLAB/SIMULINK.

Keywords—Distributed generation, distribution system, FACTS, reactive power compensation, power system stability, wind turbine induction generator.

NOMENCLATURE

Wind Turbine:

P_m	Mechanical output power of the turbine (W).
C_p	Performance coefficient of the turbine.
ρ	Air density (kg/m^3).
A	Turbine swept area (m^2).
V_{wind}	Wind speed (m/s).
λ	Tip speed ratio of the rotor blade tip speed to wind speed.
β	Blade pitch angle (deg).
P_{m_pu}	Power in pu of nominal power for particular values of ρ and A .

k_p	Power gain.
C_{P_pu}	Performance coefficient in pu of the maximum value of C_p .

Induction Machine:

R_s, L_{ls}	Stator resistance and leakage inductance.
R'_r, L'_{lr}	Rotor resistance and leakage inductance.
L_m	Magnetizing inductance.
L_s, L'_r	Total stator and rotor inductances.
V_{qs}, i_{qs}	q-axis stator voltage and current.
V'_{qr}, i'_{qr}	q-axis rotor voltage and current.
V_{ds}, i_{ds}	d-axis stator voltage and current.
V'_{dr}, i'_{dr}	d-axis rotor voltage and current.
ϕ_{qs}, ϕ_{ds}	Stator q and d-axis fluxes.
ϕ'_{qr}, ϕ'_{dr}	Rotor q and d-axis fluxes.
ω_m	Angular velocity of the rotor.
θ_m	Rotor angular position.
P	Number of pole pairs.
ω_r	Electrical angular velocity.
θ_r	Electrical rotor angular position.
T_e	Electromagnetic torque.
J	Combined rotor and load inertia coefficient.
H	Combined rotor and load inertia constant.
F	Combined rotor and load viscous friction coefficient.

I. INTRODUCTION

THE rapid development of distributed generation (DG) technology is gradually reshaping the conventional power systems in a number of countries. Wind power is among the most actively developing distributed generation. Grid-connected wind capacity is undergoing the fastest rate of growth of any form of electricity generation, achieving global annual growth rates on the order of 20 - 30% [1]. The presence of wind power generation is likely to influence the operation of the existing power system networks, especially the power system stability [2]-[3]. After the clearance of a short-circuit fault in the external

Sidhartha Panda is a research scholar in the Department of Electrical Engineering, Indian Institute of Technology, Roorkee, Uttaranchal, 247667, India. (e-mail: panda_sidhartha@rediffmail.com).

N.P.Padhy is Associate professor in the Department of Electrical Engineering, IIT, Roorkee India.(e-mail:, nppeefee@iitr.ernet.in)

network, the grid connected wind turbine should restore its normal operation without disconnection caused by inrush current and dipped voltage [4]. The protective disconnection of a large amount of wind power may cause an important loss of generation that may threaten the power system stability. Further, dynamic changes of wind speed make amount of power injected to a network highly variable. Depending on intensity and rate of changes, difficulties with frequency, voltage regulation and stability, could make a direct impact to quality level of delivered electrical energy [5]. In this context, from stability viewpoint, connection of wind turbine generator with dispersed generation of electricity, calls for a detailed technical analysis.

Majority of the wind power based DG technologies employ induction generators instead of synchronous generators, for the technical advantages of induction machines like: reduced size, increased robustness, lower cost, and increased electromechanical damping. Wind turbine induction generator (WTIG) can be viewed as a consumer of reactive power. Its reactive power consumption depends on active power production. Further, induction generators draw very large reactive currents during fault occurrence [6]. Following the fault conditions, the voltage recovery may become impossible, and consequently the wind farm may experiences voltage collapse at its terminals. One way to prevent this from happening is by providing reactive power compensation which would help in preventing the voltage collapse at the terminals of wind farms, which would lead to improving the stability of the wind farm. Conventionally, shunt capacitor banks are connected at the generator terminals to compensate its reactive power consumption.

To minimize reactive power exchange between wind power plant and distribution network, dynamic compensation of reactive power can be employed [7]-[8]. Further, the normal operation restoration after the clearance of an external system fault can be improved with dynamic reactive compensation. Without the dynamic compensation, it is possible that at some locations only a small number of wind turbines could be connected due to weak voltage conditions. This would not only leave assessed wind potential unused, but it could also prohibit installation of larger number of wind turbines jeopardizing the economics of the whole project. Recent development of power electronics introduces the use of flexible ac transmission system (FACTS) controllers in power systems [9]. Shunt FACTS devices play an important role in controlling the reactive power flow in the power network, which in turn affects the system voltage fluctuation and transient stability. The STATCOM is one of the important FACTS devices and can be used for dynamic reactive power compensation of power systems to provide voltage support and stability improvement [10].

In this work the effect of a STATCOM in improving the stability performance of the distributed network with WTIG is studied. In order to overcome negative dynamic impacts caused by WTIGs, a STATCOM is used at the point of WTIGs and distribution network connection. The study is based on the three phase non-linear dynamic simulation, utilizing the SimPowerSystem blockset for use with MATLAB/SIMULINK [11]. Simulation results are presented to show the improved stability performance of a distributed network embedded with WTIGs under severe

disturbances with the use of a STATCOM. Further the effects different types of wind speed and different control mode of operation of STATCOM on distribution system are presented.

II. DISTRIBUTION SYSTEM COMPONENTS MODELS

Distribution systems are inherently unbalanced due to the asymmetrical line spacing and imbalance of customer load. In view of this, single phase models can not be used for accurate studies on the operation of distributed systems. Therefore in this work all network components are represented by the three-phase models [11].

A. Wind Turbine Induction Generator (WTIG)

The block diagram of wind turbine the induction generator (WTIG) is shown in Fig. 1. The stator winding is connected directly to the 60 HZ grid and the rotor is driven by a variable-pitch wind turbine. The power captured by the wind turbine is converted into electrical power by the induction generator and is transmitted to the grid by the stator winding. The pitch angle is controlled in order to limit the generator output power to its nominal value for high wind speeds. In order to generate power the induction generator speed must be slightly above the synchronous speed.

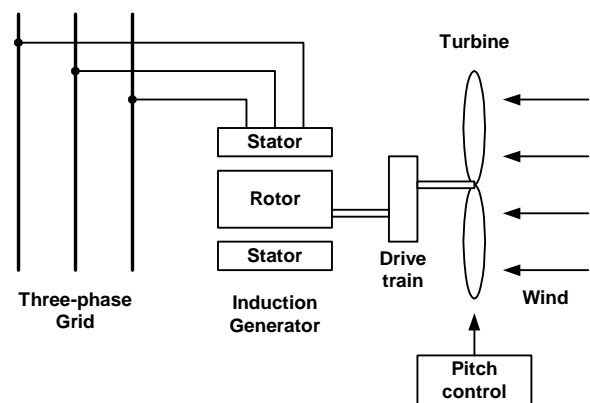


Fig. 1 Block diagram of wind turbine with induction generator

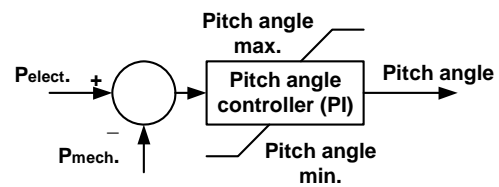


Fig. 2 Control system for pitch angle control.

The pitch angle controller regulates the wind turbine blade pitch angle β , according to the wind speed variations. Hence, the power output of WTIG depends on the characteristics of the pitch controller in addition to the turbine and generator characteristics. This control guarantees that, irrespective of the voltage, the power output of the WTIG for any wind speed will be equal to the designed value for that speed. This designed power output of the WTIG with wind speed is provided by the manufacturer in the form of a power curve. Hence, for a

given wind speed, power output can be obtained from the power curve of the WTIG.

A Proportional-Integral (PI) controller is used to control the blade pitch angle in order to limit the electric output power to the nominal mechanical power. The pitch angle is kept constant at zero degree when the measured electric output power is under its nominal value. When it increases above its nominal value the PI controller increases the pitch angle to bring back the measured power to its nominal value. The pitch angle control system is illustrated in the Fig. 2. The pitch angle is controlled in order to limit the generator output power at its nominal value for winds exceeding the nominal speed. In order to generate power the IG speed must be slightly above the synchronous speed. Speed varies approximately between 1 pu at no load and 1.005 pu at full load. Each wind turbine has a protection system monitoring voltage, current and machine speed.

1) Wind Turbine

The wind turbine model is employed in the present study is based on the steady-state power characteristics of the turbine. The stiffness of the drive train is infinite and the friction factor and the inertia of the turbine are combined with those of the generator coupled to the turbine. The wind turbine mechanical power output is a function of rotor speed as well as the wind speed and is expressed as:

$$P_m = C_P(\lambda, \beta) \frac{\rho A}{2} V_{wind}^3 \quad (1)$$

Normalizing (1) in the per unit (pu) system as:

$$P_{m_pu} = k_p C_{P_pu} V_{wind_pu}^3 \quad (2)$$

A generic equation is used to model $C_P(\lambda, \beta)$. This equation, based on the modeling turbine characteristics is [11]:

$$C_P(\lambda, \beta) = c_1 \left(\frac{c_2}{\lambda_i} - c_3 \beta - c_4 \right) e^{\frac{-c_5}{\lambda_i}} + c_6 \lambda \quad (3)$$

With

$$\frac{1}{\lambda_i} = \frac{1}{\lambda + 0.08 \beta} - \frac{0.035}{\beta^3 + 1} \quad (4)$$

The relevant parameters are given in appendix

2) Induction Machine

In the present study, the electrical part of the machine is represented by a fourth-order state-space model and the mechanical part by a second-order system. All electrical variables and parameters are referred to the stator. All stator and rotor quantities are in the arbitrary two-axis reference frame (d-q frame). The d-axis and q-axis block diagram of the electrical system is shown in Figs. 3 (a) and 3 (b).

The electrical equations are given by:

$$v_{qs} = R_s i_{qs} + \frac{d}{dt} \varphi_{qs} + \omega \varphi_{ds} \quad (5)$$

$$v_{ds} = R_s i_{ds} + \frac{d}{dt} \varphi_{ds} - \omega \varphi_{qs} \quad (6)$$

$$v'_{qr} = R'_r i_{qr} + \frac{d}{dt} \varphi'_{qr} + (\omega - \omega_r) \varphi'_{dr} \quad (7)$$

$$v'_{dr} = R'_r i_{dr} + \frac{d}{dt} \varphi'_{dr} - (\omega - \omega_r) \varphi'_{qr} \quad (8)$$

$$T_e = 1.5 p (\varphi_{ds} i_{qs} - \varphi_{qs} i_{ds}) \quad (9)$$

Where,

$$\varphi_{qs} = L_s i_{qs} + L_m i'_{qr}$$

$$\varphi_{ds} = L_s i_{ds} + L_m i'_{dr}$$

$$\varphi'_{qr} = L'_r i'_{qr} + L_m i_{qs}$$

$$\varphi'_{dr} = L'_r i'_{dr} + L_m i_{ds}$$

With $L_s = L_{ls} + L_m$ and $L'_r = L'_{lr} + L_m$

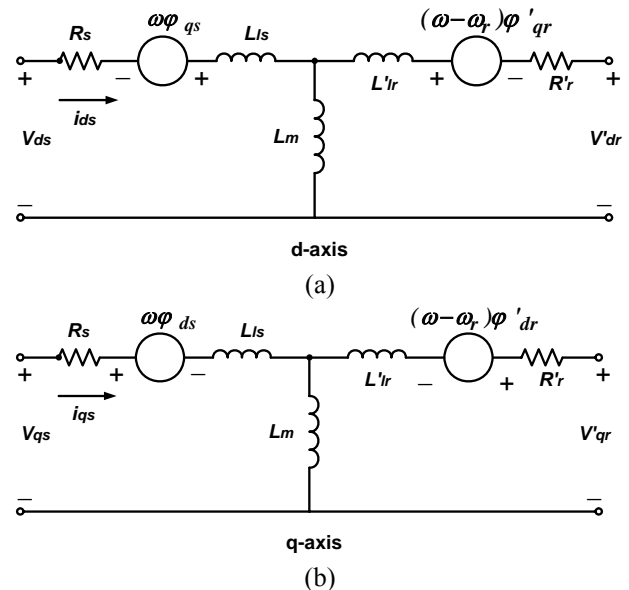


Fig. 3 Induction machine equivalent circuits (a) d-axis equivalent circuit (b) q-axis equivalent circuit.

The mechanical equations are given by:

$$\frac{d}{dt} \omega_m = \frac{1}{2H} (T_e - F \omega_m - T_m) \quad (10)$$

$$\frac{d}{dt} \theta_m = \omega_m \quad (11)$$

B. Protection System

Commercial wind turbines incorporate sophisticated system for protection of electrical and mechanical components. These turbine-based protection system respond

to local conditions, detecting grid or mechanical anomalies that indicate system trouble or potentially damaging conditions for the turbine. The protection system should respond almost instantaneously to mechanical speed, vibration, voltages, or currents outside of defined tolerances. In addition, conventional multi-function relays for electric machine protection should also be provided to detect a wide variety of grid disturbances and abnormal conditions within the machine. In the present study the WTIG protection system consists of the followings:

- Instantaneous/positive-sequence AC Overcurrent.
- AC Current Unbalance.
- AC Overvoltage/Undervoltage (positive-sequence).
- AC Voltage Unbalance (Negative-sequence / Zero-sequence).
- DC Overvoltage.

C. Static Synchronous Compensator (STATCOM)

The STATCOM is based on a solid state synchronous voltage source, which generates a balanced set of three sinusoidal voltages at the fundamental frequency, with rapidly controllable amplitude and phase angle. The STATCOM block used in the present study, models an IGBT-based STATCOM. However, as details of the inverter and harmonics are not represented in stability studies, a GTO-based model can also be used. Fig. 4 shows a single-line diagram of the STATCOM and a simplified block diagram of its control system. The control system consists of:

- A phase-locked loop (PLL) to synchronize on the positive-sequence component of the three-phase primary voltage V_1 . The direct-axis and quadrature-axis components of the AC three-phase voltage and currents (labeled as V_d , V_q or I_d , I_q on the diagram) are computed using the output of the PLL.
- The measurement systems measuring the d-axis and q-axis components of AC positive-sequence voltage and currents to be controlled and the DC voltage V_{dc} .
- The regulation loops, namely the AC voltage regulator and a DC voltage regulator. The output of the AC voltage regulator and DC voltage regulator are the reference current $I_{q\text{ref}}$ and $I_{d\text{ref}}$, for the current regulator.
- An inner current regulation loop consisting of a current regulator, which controls the magnitude and phase of the voltage generated by the PWM converter.

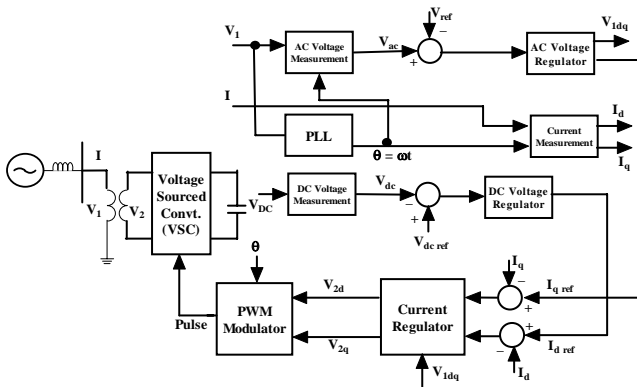


Fig. 4 Single-line diagram of control system of STATCOM

III. SYSTEM UNDER STUDY

The one line diagram of the test system employed in this study is shown in Fig. 5. The network consists of a 120-kv, 60-Hz, sub-transmission system with short circuit level of 2500 MVA, feeds a 25 kv distribution system through 120/25 kv step down transformers. A wind farm consisting of six 1.5-MW wind turbines is connected to the 25-kV distribution system, exports power to the 120-kV grid through a 25-km 25-kV feeder. Very large reactive currents are drawn by IGs during fault conditions and hence reactive power compensation is provided. Part of the reactive power consumed by the induction generators is locally supplied by fixed capacitors of 400 kVAr each, installed at the terminals of the machines. Dynamic reactive power compensation is provided by a 3 MVA STATCOM located at the point of WTIGs connection to the distribution network (bus 3). Both WTIG and STATCOM used in the present study are phasor models which are valid for transient stability solution.

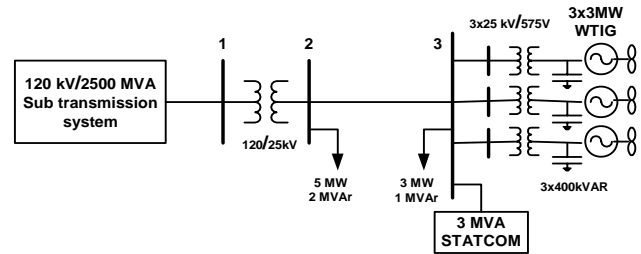


Fig. 5 Single-line diagram of the distribution system embedded with wind turbine induction generators and a STATCOM.

Wind turbines use squirrel-cage induction generators. The stator winding is connected directly to the 60 Hz grid and the rotor is driven by a variable-pitch wind turbine. In order to limit the generator output power at its nominal value, the pitch angle is controlled for winds exceeding the nominal speed of 9 m/s. To inject active power to the distribution network, the IG speed must be slightly above the synchronous speed. Speed varies approximately between 1 pu at no load and 1.005 pu at full load. Each wind turbine has a protection system monitoring voltage, current and machine speed. All the relevant data are given in appendix. Therefore, the amount of active power injected by WTIGs to the distribution system is limited by transient stability issues. Alternatively, as long as the WTIGs inject active power to the distribution network, transient stability is maintained [4].

IV. SIMULATION RESULTS

The dynamic behavior of the WTIGs during an external three-phase fault is analyzed and presented in this section. The active power generated by the WTIGs depends upon the wind speed. Two type of wind speed namely; constant wind speed and linear change of wind speed, are considered in the present study as shown in Fig. 6. Further, the reference voltage and the reference reactive power are set to 1 pu for both voltage controlled mode and VAR controlled mode.

Three cases are considered for all the types of wind speed changes:

Case-1: System without STATCOM.

Case-2: System with STATCOM, operating in the voltage control mode of operation.

Case-3: System with STATCOM, operating in the VAR/power factor control mode of operation.

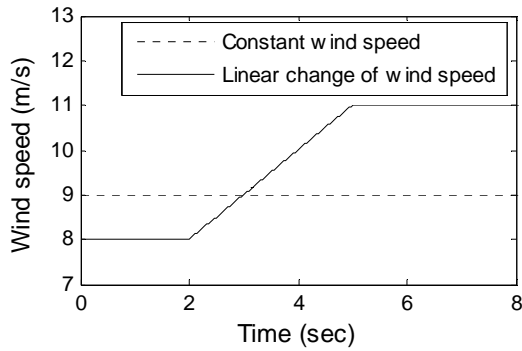


Fig. 6 Types of wind speed

A. Constant Wind Speed

A constant wind speed of 9 m/s is applied to the wind turbine. A three phase fault is applied at the bus no. 3, at $t=2$ sec. and cleared after 9 cycles. The original system is restored upon the fault clearance. Three cases as mentioned above are analyzed. Fig. 7 shows the response of WTIG terminal voltage for the above contingency.

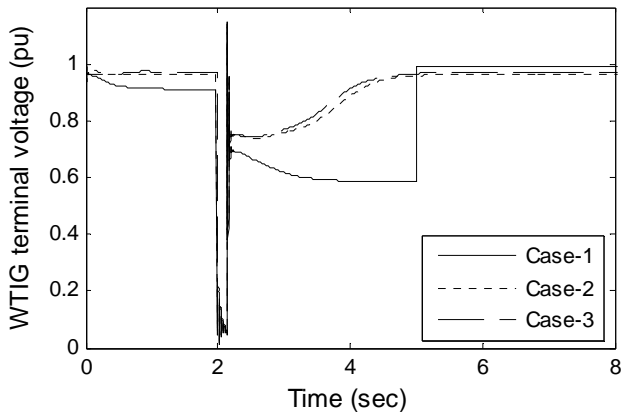


Fig. 7 WTIG terminal voltage response for a 9 cycle 3-phase fault

It can be seen from Fig. 7 that, as the fault is applied near to the WTIGs (bus-3), the WTIG terminal voltage drops drastically on the occurrence of the fault. The low voltage condition starts at $t=2$ sec, at which the fault is applied and lasts for 9 cycles i.e. the duration of the fault. For case of system without STATCOM (shown in Fig. 7, with legend Case-1), the WTIG terminal voltage drops to 0.69 pu immediately after the fault clearance. The AC Undervoltage limit set by the protection system being equal to 0.75 pu, this low voltage condition results in tripping of WTIGs at $t=5$ s, the tripping being initiated by the AC Undervoltage protection. For the system with STATCOM

(shown in Fig. 7, with legends Case-2 & 3), because of reactive power support, the WTIG terminal voltage is slightly more than 0.75 pu immediately after the fault clearance, and is within the limit set by the protection system. So the system maintains stability and finally the WTIG terminal voltage recovers close to 1 pu for both the cases. Further, it can be seen from Fig. 7 that, for the case of STATCOM operating in VAR control mode (Case-3), the terminal voltage is slightly more than 1 pu as the controller tries to supply the rated reactive power. But, when the STATCOM is operating in voltage control mode (Case-2), the controller tries to maintain the terminal voltage constant at the set value of 1 pu and the STATCOM supplies that much reactive power as is required to maintain the terminal voltage constant.

The response of the active power injected into the network is shown in Fig. 8. The active power injected to the distribution network reduces drastically during the duration of fault for all the cases. For the case of system without STATCOM (Case-1), because of the tripping of the WTIGs, the active power injected becomes zero after the fault clearance. But, for the cases of system with STATCOM (shown in Fig. 8, with legends Cases- 2 & 3), because of the reactive power support, the stability of the system is maintained and the WTIGs continue to supply the rated power to the distribution network after the fault clearance.

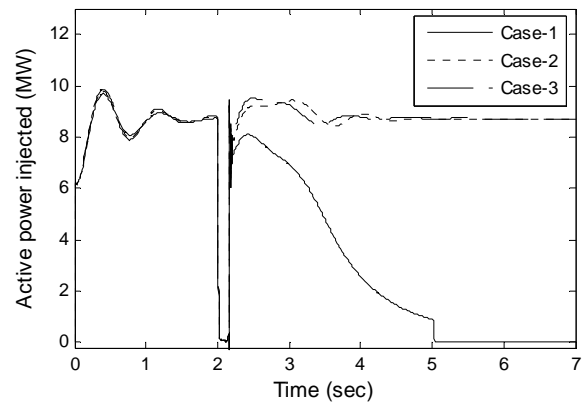


Fig. 8 Response of active power injected to the network for a 9 cycle 3-phase fault

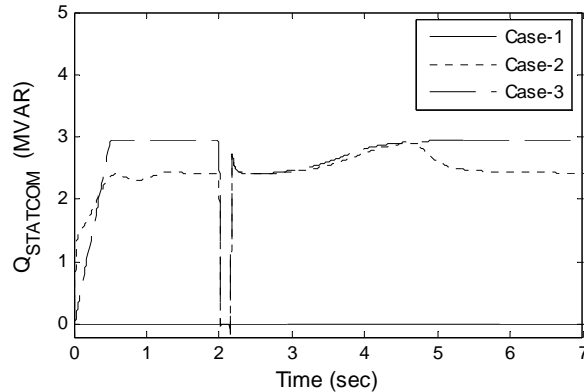


Fig. 9 Reactive power supplied by the STATCOM

Fig. 9 shows the variation of the reactive power supplied by the STATCOM for the above contingency, for all the cases. When the STATCOM is inactive (shown in Fig. 9,

with legend, Case-1), the reactive power supplied by it is obviously zero. It is also clear from Fig. 9 that, for the case of STATCOM operating in voltage control mode (shown in Fig. 9, with legends Case-2), the controller tries to maintain the terminal voltage constant at the set value of 1 pu and consequently the STATCOM supplies that much reactive power as is required to maintain the terminal voltage constant. In case of STATCOM operating in VAR control mode (shown in Fig. 9, with legends Case-3), as the reference reactive power is set to 1 pu, the controller tries to supply the rated reactive power. Hence the reactive power supplied for Case-3 is more than that of Case-2.

The response of WTIG speed is shown in Fig. 10. The speed of the WTIGs increases at the occurrence of the fault at $t=0.2$ sec, for all the cases. For the case of system without STATCOM (Case-1), as explained earlier, the system loses stability and the speed of the WTIGs continues to increase. For the system with STATCOM (shown in Fig. 10, with legends Case-2 & 3), the stability of the system is maintained after the fault clearance. Further, it can be seen from Fig. 10 that the WTIG speed for Case-2 is slightly more than that for Case-3. This is due to the fact that, the reactive power supplied by the STATCOM is more in Case-3, compared to the Case-2. In Case-2, the WTIGs draw the difference reactive power from the distribution network and hence the WTIGs are slightly overloaded compared to Case-3.

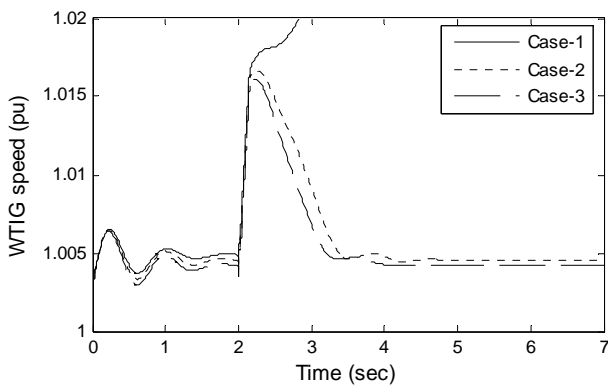


Fig. 10 Response of WTIG speed

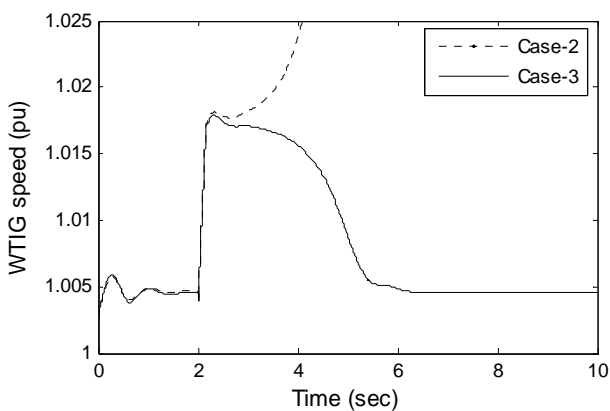


Fig. 11 Response of WTIG speed for different control modes of operation of STATCOM

To compare the performance of two modes of operation on transient stability improvement, the fault clearing time is increased by half a cycle and the same contingency is

simulated. The response of WTIG speed is shown in Fig. 11. It can be seen from Fig. 11 that, when the STATCOM is operating in voltage control mode (shown in Fig. 11 with legend Case-2), the system loses stability due to the tripping of the WTIGs by the protection system. In case of STATCOM operating in VAR control mode (shown in Fig. 11 with legend Case-3), stability of the system is maintained. The difference between the reactive power requirement of the WTIGs and the reactive power supplied by the STATCOM is drawn from the distribution network. As explained earlier, the reactive power supplied by the STATCOM is more in Case-3, compared to the Case-2. In order to meet the reactive power requirement, the WTIGs are slightly overloaded in Case-2 compared to the Case-3. Hence, VAR control mode of operation of STATCOM improves the stability compared to the voltage control mode of operation.

B. Linear Change of Wind Speed

A linear change of wind speed as shown in Fig. 6 is applied to the wind turbine. This type of wind speed change enables the wind turbine to inject active power into a network from minimum to maximum value in a manner slow enough not to induce unwanted oscillations. As the maximum wind speed reaches 11 m/s, the active power injected to the network increases to 9.0 MW compared to constant wind speed (9 m/s) generation of 8.71 MW. The reactive power requirement of WTIG increases with the increase in the active power generation.

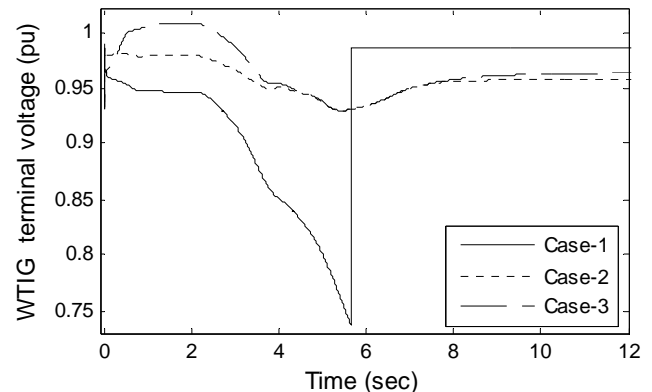


Fig. 12 Response of WTIG terminal voltage for linear change of wind speed

Fig. 12 shows the response of the WTIG terminal voltage (without fault), for all the cases. For the case of system without STATCOM (shown in Fig. 12, with legends Case-1), the WTIG terminal voltage drops below 0.75 pu, due to the insufficient reactive power compensation. This low voltage value is less than the AC Undervoltage limit of 0.75 pu, set by the protection system. This low voltage condition results in tripping of WTIGs at $t=5$ s, the tripping being initiated by the AC Undervoltage protection. Hence the stability of the system is lost for Case-1. For the system with STATCOM (shown in Fig. 12, with legends Case-2 & 3), the WTIG terminal voltage improves to 0.92 pu because of reactive power support. This is well within the limit set by the protection system. So the system stability is maintained and finally the WTIG terminal voltage recovers close to 0.95 pu for both the cases. Further, it can also be

seen from Fig. 12 that, for the case of STATCOM operating in VAR control mode (Case-3), the terminal voltage is slightly more than that of STATCOM operating in voltage control mode (Case-2). As explained earlier, this is due to the fact that the reactive power supplied by the STATCOM is more in Case-3 than the Case-2. In Case-2, the WTIGs draw more reactive power from the distribution network and hence the WTIGs are slightly overloaded compared to Case-3.

To compare the performance of two modes of operation on improving the stability, a three phase fault of 5 and half cycle duration is applied at the bus no. 3, at $t=12$ sec. The original system is restored upon the fault clearance. The response of the WTIG speed is shown in Fig. 13. In the pre-fault period, the WTIG speed settles to around 1.005 pu after the initial transients. The WTIG speed increases drastically at the occurrence of the fault at $t=12$ sec, for both the cases. It can be seen from Fig. 13 that, when the STATCOM is operating in voltage control mode (shown in Fig. 13 with legend Case-2), the system stability is lost due to the tripping of the WTIGs by the protection system. As explained earlier and shown in Fig. 12, the WTIG terminal voltage in Case-2 is slightly less than that of Case-3. Hence the WTIG terminal voltage drops to a lower value in Case-2 compared to Case-3, upon the occurrence of the fault. This low voltage condition results in tripping of the WTIGs for Case-2. The tripping is initiated by the AC Undervoltage protection. In case of STATCOM operating in VAR control mode (shown in Fig. 13 with legend Case-3), stability of the system is maintained. This is due to the fact that, in Case-3 the pre-fault WTIG terminal voltage was comparatively higher, and upon the occurrence of the fault, drops to a value within the limit set by the protection system. Hence stability of the system is maintained in Case-3.

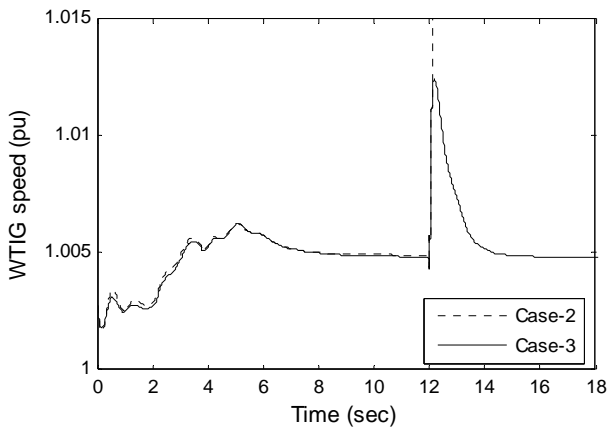


Fig. 13 Response of WTIG speed for different control modes of STATCOM

The response of the active power injected into the distribution network is shown in Fig. 14, for the same contingency and for both the cases. As the linear change of wind speed from 8 to 11 m/s is applied to the wind turbines, the active power injected to the distribution network increases with the increase in wind speed. After the initial transients the active power injected to the distribution network finally settles to its rated value of 9 MW. As the fault is applied at $t=12$ sec., near the WTIG bus (bus-3), the active power injected to the distribution network reduces

drastically during the fault duration for both the cases. As explained earlier, the low voltage condition in Case-2 results in tripping of the WTIGs, upon the clearance of the fault. Hence, the active power injected to the distribution network becomes zero (shown in Fig. 14, with legends Case-2). In case of STATCOM operating in VAR control mode, due to the higher pre-fault WTIG terminal voltage, stability of the system is maintained upon the clearance of the fault (shown in Fig. 14 with legend Case-3).

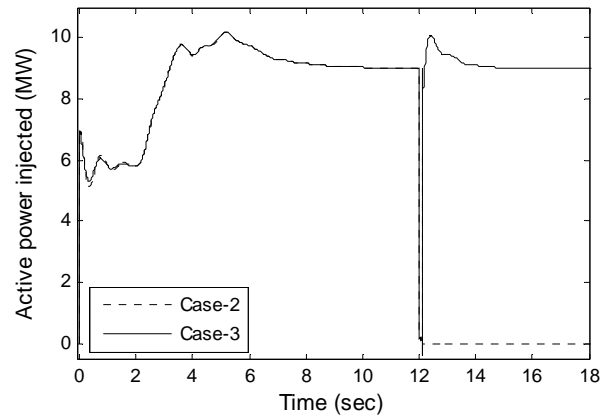


Fig. 14 Response of active power injected to the network for different control modes of STATCOM

V. CONCLUSION

This paper presented a study about the stability improvement of a distribution system embedded with wind farms. For dynamic reactive power compensation, a FACTS-based controller is employed. The dynamic behavior of the example distribution system, during an external three-phase fault and under various types of wind speed changes, is investigated. Simulation results show that the FACTS-based reactive power compensation prevents large deviations of bus voltage magnitude induced by reactive power drawn from distribution network by WTIGs.

It is observed that, for the case of FACTS controller operating in voltage control mode, the controller tries to maintain the terminal voltage constant, at its preset reference value of 1 pu. Consequently the FACTS controller supplies that much reactive power as is required to maintain the voltage constant. For the case of FACTS controller operating in VAR control mode the controller tries to supply the preset reference reactive power of 1 pu and hence tries to supply the rated reactive power. As the reactive power supplied for VAR control mode is more than that of voltage control mode, the VAR control mode of operation of FACTS controller is more effective in improving the stability of the system compared to the voltage control mode of operation.

APPENDIXES

Example distribution system data (All data are in pu unless specified otherwise; the notations used are defined in [11]).

Transformer parameters:

Substation: 47 MVA, 120/25 kV, $R_2=0.0026$, $L_2=0.08$, $R_m=500\Omega$, $X_m=500\Omega$.

WTIG to distribution network: Each 4 MVA, 25 kV/575 V,
 $R_2=0.0008$, $L_2=0.025$, $R_m=500\Omega$, $X_m=inf$.

Transmission line parameters per km: $R_1=0.1153 \Omega$,
 $R_0=0.413 \Omega$, $L_1=1.05 \text{ mH}$, $L_0=3.32 \text{ mH}$, $C_1=11.33 \text{ nF}$,
 $C_0=5.01 \text{ nF}$.

STATCOM parameters: 25 kV, MVA, $R=0.071$, $L=0.22$,
 $V_{dc}=4\text{KV}$, $C_{dc}=0.0011 \text{ F}$, Regulator gains: V_{ac} - $K_p=5$ &
 $K_i=1000$, V_{dc} - $K_p=0.0001$ & $K_i=0.02$, I - $K_p=0.3$, $K_i=10$ &
 $K_f=0.22$, $Droop=0.03$.

WTIG parameters:

Turbine: Each- 3 MW, base wind speed =9 m/s, β controller
 $K_p=5$, $K_i=25$, $\max \beta =45^\circ$.

Generator: Each- $P=3.33 \text{ MVA}$, $V=575\text{V}$, $f=60 \text{ Hz}$, $R_s=$
 0.004843 , $L_s=0.1248$, $R_r'=0.004377$, $L_r'=0.1791$, $L_m=6.7$,
 $H=5.04$, $F=0.01$, $p=3$.

dynamic stability, FACTS, optimization techniques, distributed generation and wind energy.

Narayana Prasad Padhy was born in India and received his Degree (Electrical Engineering), Masters Degree (Power Systems Engineering) with Distinction and Ph.D., Degree (Power Systems Engineering) in the year 1990, 1993 and 1997 respectively in India. Then he has joined the Department of Electrical Engineering, Indian Institute of Technology (IIT) India, as a Lecturer, Assistant Professor and Associate Professor during 1998, 2001 and 2006 respectively. Presently he is working as an Associate Professor in the Department of Electrical Engineering, Indian Institute of Technology (IIT) India. He has visited the Department of Electronics and Electrical Engineering, University of Bath, UK under Boyscast Fellowship during 2005-06. His area of research interest is mainly Power System Privatization, Restructuring and Deregulation, Transmission and Distribution network charging, Artificial Intelligence Applications to Power System and FACTS.

REFERENCES

- [1] OECD/IEA, Wind Power Integration into Electricity Systems, Case Study 5, [Online]. Available: <http://www.oecd.org/env/cc/>
- [2] F. Jurado and J. Carpio, "Enhancing the distribution networks stability using distributed generation," *The International Journal for Computation and Mathematics in Electrical and Electronic Engineering*, vol. 24, no. 1, 2005, pp. 107-26.
- [3] Vijay Vittal, "Consequence and impact of electric utility industry restructuring on transient stability and small-signal stability analysis," *IEEE Proceedings*, vol. 88, no. 2, 2000, pp. 196-207.
- [4] O. Samuelsson and S. Lindahl, "On speed stability," *IEEE Trans. Power Sys.*, vol. 20, no. 2, 2005, pp. 1179 – 1180.
- [5] N. D. Hatziaargyriou and A. P. S. Meliopoulos, "Distributed energy sources: technical challenges," *IEEE Power Engineering Society Winter Meeting*, vol. 2, 2002, pp. 1017 – 1022.
- [6] R. Gnativ and J. V. Milanovi, "Voltage sag propagation in systems with embedded generation and induction motors," *IEEE Power Engineering Society Summer Meeting*, vol. 1, 2001, pp. 474 – 479.
- [7] N. Dizdarevic, M. Majstrovic and G. Andersson, "Reactive power compensation of wind energy conversion system by using Unified Power Flow Controller," *Int. J. Energy Technology and Policy*, vol. 3, no. 3, 2005, pp. 269-298.
- [8] W. Freitas, E. Asada, A. Morelato and Xu Wilsun, "Dynamic improvement of induction generators connected to distribution systems using a DSTATCOM," *Proceedings, International Conference on Power System Technology, PowerCon*, vol. 1, 2002, pp. 173 – 177.
- [9] N. G. Hingorani and L. Gyugyi, *Understanding FACTS: Concepts and Technology of Flexible AC Transmission System*. IEEE Press. 2000.
- [10] L. Gyugyi, 'Dynamic Compensation of AC Transmission Lines by Solid-state Synchronous Voltage Sources', *IEEE Trans. on Power Delivery*, vol. 9, no. 2, 1994, pp. 904 – 911.
- [11] SimPowerSystems User guide. Available <http://www.mathworks.co>

Sidhartha Panda received the M.E. degree in Power Systems Engineering from University College of Engineering, Burla, Sambalpur University, India in 2001. Currently, he is a Research Scholar in Electrical Engineering Department of Indian Institute of Technology Roorkee, India. He was an Associate Professor in the Department of Electrical and Electronics Engineering, VITAM College of Engineering, Andhra Pradesh, India and Lecturer in the Department of Electrical Engineering, SMIT, Orissa, India. His areas of research include power system transient stability, power system